Hindawi Publishing Corporation
Advances in Condensed Matter Physics
Volume 2015, Article ID 594176, 9 pages
http://dx.doi.org/10.1155/2015/594176

Hindawi

Research Article

Hydrostatic Pressure and Built-In Electric Field Effects on the Donor Impurity States in Cylindrical Wurtzite GaN/$Al_xGa_{1-x}N$ Quantum Rings

Guangxin Wang,[1] Xiuzhi Duan,[2] and Rui Zhou[1]

[1]*College of Science, Hebei United University, Tangshan 063000, China*
[2]*College of Light Industry, Hebei United University, Tangshan 063000, China*

Correspondence should be addressed to Guangxin Wang; guangxinwang@126.com

Received 18 December 2014; Accepted 29 January 2015

Academic Editor: David Huber

Within the framework of the effective mass approximation, the ground-state binding energy of a hydrogenic impurity is investigated in cylindrical wurtzite GaN/$Al_xGa_{1-x}N$ strained quantum ring (QR) by means of a variational approach, considering the influence of the applied hydrostatic pressure along the QR growth direction and the strong built-in electric field (BEF) due to the piezoelectricity and spontaneous polarization. Numerical results show that the donor binding energy for a central impurity increases inchmeal firstly as the QR radial thickness (ΔR) decreases gradually and then begins to drop quickly. In addition, the donor binding energy is an increasing (a decreasing) function of the inner radius (height). It is also found that the donor binding energy increases almost linearly with the increment of the applied hydrostatic pressure. Moreover, we also found that impurity positions have an important influence on the donor binding energy. The physical reasons have been analyzed in detail.

1. Introduction

In recent years, nitride-based wurtzite semiconductor materials AlN, GaN, and InN and their alloys have been widely studied due to their promising applications in optoelectronic devices such as light-emitting devices and laser diodes [1–3]. The electronic and optical properties of various confined systems such as quantum wells [4–8], quantum well wires [9, 10], and (double) quantum dots [11–15] can be changed by doped impurities. Therefore, many theoretical investigations concerning the impurity states have been done in semiconducting nanostructures by well-known approaches such as variational approach [4–15], strong confinement approach [16, 17], and perturbation approach [18]. As expected, the hydrostatic pressure applied on a bulk material can not only modify the parameters, such as the band gaps, the potential barriers, the conduction effective masses, the static dielectric constants, and the lattice constants, but also change the dimension of the low-dimensional systems, which is associated with the fractional change in the volume. Moreover, the strong built-in electric field also affects obviously the electric and optical properties of the wurtzite nitride-based quantum heterostructures. According to the above characteristics, the hydrogenic donor impurity states in QWs (QWWs) [4–10] have been extensively studied under the influence of the electric and magnetic fields. Various studies [11, 12, 19–22] related to the effects of hydrostatic pressure and built-in electric field on the donor binding energy in QDs have also been reported.

Since the first GaAs/$Al_xGa_{1-x}As$ quantum ring (QR) of nanoscopic sizes was fabricated [22, 23] and exhibited fascinating behaviors such as interesting electronic and optical properties. The electronic structure and optical properties of arsenic based QR under external influences have been extensively studied. Li and Xia [24, 25] studied the electronic states of InAs/GaAs QR (GaAs/$Al_xGa_{1-x}As$ DQR) in the frame of effective mass envelope function theory by employing the matrix diagonalization method. The papers show that the electron energy levels are sensitively dependent on the radial thickness, the height of the QR (DQR), and

the magnetic field strength. Except for the energy levels of the carriers, other effects can be obtained in the QR, such as the Aharonov-Bohm oscillation induced by the magnetic field [26]. On the other hand, a theoretical study of shallow donor states in GaAs-(Ga,Al)As QRs, within the effective mass approximation and using a variational method, which is presented in [27]. The explicit dependencies of the impurity binding energy on the magnetic field strength, the structure parameters of the QR, and the impurity positions are obtained. In addition, considering the effects of hydrostatic pressure, temperature, aluminum concentration, and impurity position, Baghramyan et al. [28] investigated the binding energy of hydrogenic donor impurity in GaAs/$Ga_{1-x}Al_xAs$ concentric double quantum rings. And Monozon and Schmelcher [29] have studied the problem of an impurity in a QR in the presence of a radially directed strong external electric field by means of the analytical and numerical approaches. On the other hand, Barseghyan and coworkers [30, 31] have investigated the behavior of the binding energy and photoionization cross section of a hydrogenic-like donor impurity in InAs quantum ring with Pöschl-Teller confinement potential along the axial direction by using the variational method. In the above papers, the combined effects of hydrostatic pressure and electric and magnetic fields applied in the growth direction have been taken into account. Moreover, we [32] also studied the hydrogenic impurity binding energy in GaAs/$Al_xGa_{1-x}As$ QR under the external electric field in finite potential barrier by means of a variational approach.

As far as we know, there are no reports on the hydrostatic pressure and built-in electric field (BEF) effects on the donor binding energy in wurtzite GaN/$Al_xGa_{1-x}N$ strained QR to date. Therefore, it is very necessary to investigate the donor impurity states in wurtzite GaN/$Al_xGa_{1-x}N$ strained QR. In our work, the effects of hydrostatic pressure, impurity positions, and sizes of the structure on the donor binding energy in wurtzite GaN/$Al_xGa_{1-x}N$ strained QR are investigated by means of a variational approach. The paper is organized as follows. In Section 2 we describe the theoretical framework. Section 3 is dedicated to the results and discussions, and our conclusions are given in Section 4.

2. Theoretical Framework

2.1. Hamiltonian and Impurity States. In Figure 1, the schematic view of a cylindrical wurtzite GaN/$Al_xGa_{1-x}N$ QR is depicted, with a detailed description of the different dimensions of the QR (inner radius R_1, outer radius R_2, height L_w, and the QR radial thickness ΔR). Additionally, the GaN ring is embedded in a $Al_xGa_{1-x}N$ host matrix material, and the z-axis is defined to be the QR growth direction. Within the frame of the effective mass approximation, the Hamiltonian for a hydrogenic donor impurity in cylindrical wurtzite GaN/$Al_xGa_{1-x}N$ QR under the influence of hydrostatic pressure can be written as

$$\widehat{H} = \widehat{H}_0 - \frac{e^2}{4\pi\varepsilon_0\overline{\varepsilon}(p)\left|\vec{r} - \vec{r}_0\right|}, \tag{1}$$

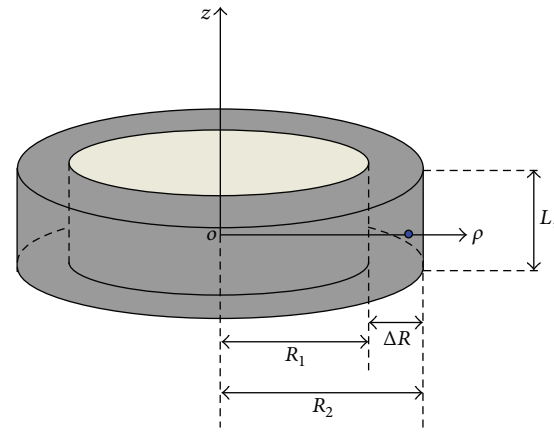

Figure 1: The diagram of a cylindrical wurtzite GaN/$Al_xGa_{1-x}N$ QR.

where $\vec{r}(\vec{r}_0)$ denotes the position vector of the electron (impurity ion), e is the absolute value of the electron charge, ε_0 is the permittivity of free space, and $\overline{\varepsilon}(p)$ is the pressure-dependent effective mean relative dielectric constant of GaN and $Al_xGa_{1-x}N$ materials. The Hamiltonian $\widehat{H}_0$ is given by [11]

$$\widehat{H}_0 = -\frac{\hbar^2}{2m_\perp(p)}\left(\frac{1}{\rho}\frac{\partial}{\partial\rho}\left(\rho\frac{\partial}{\partial\rho}\right) + \frac{1}{\rho^2}\frac{\partial^2}{\partial\varphi^2}\right) - \frac{\hbar^2}{2m_{/\!/}(p)}\frac{\partial^2}{\partial z^2} + V(\rho, z, p) - eF_{w,b}(p)\,z, \tag{2}$$

where $m_{/\!/}$ and $m_\perp$ are the pressure-dependent effective mass of the electron along and perpendicular to the [0001]-direction. In (2), $F(p)$ is the pressure-dependent BEF in the finitely thick barrier layer. The values of the BEF along the QR growth direction in the ring ($F_{\mathrm{GaN}}(p)$) and the barrier ($F_{\mathrm{Al}_x\mathrm{Ga}_{1-x}\mathrm{N}}(p)$), which results from the difference in the total electric polarizations in each region, are given by simple formulas [14] as follows:

$$F_{\mathrm{GaN}}(p) = \left|\frac{L_b\left(P_{sp}^{\mathrm{AlGaN}} + P_{pe}^{\mathrm{AlGaN}} - P_{sp}^{\mathrm{GaN}} - P_{pe}^{\mathrm{GaN}}\right)}{\varepsilon_0\left(L_b\varepsilon_e^{\mathrm{GaN}} + L_w\varepsilon_e^{\mathrm{GaN}}\right)}\right|,$$
$$F_{\mathrm{AlGaN}}(p) = -\frac{L_w}{L_b}F_{\mathrm{GaN}}(p), \tag{3}$$

where L_w is the QR height and L_b is the thickness of the barrier layer along the QR growth direction. $\varepsilon_e^{\mathrm{GaN}}$ ($\varepsilon_e^{\mathrm{AlGaN}}$) is the dielectric constant for GaN ($Al_xGa_{1-x}N$) material; P_{sp}^{GaN}, P_{sp}^{AlGaN} and P_{pe}^{GaN}, P_{pe}^{AlGaN} are the spontaneous and piezoelectric polarizations for GaN and $Al_xGa_{1-x}N$ materials. And $V(\rho, z, p)$ is the electron confinement potential due to the band offset ($Q_j = 0.765$) and is given by

$$V(\rho, p) = \begin{cases} 0, & R_1 \le R \le R_2, \\ Q_j\left[E_{g,\mathrm{Al}_x\mathrm{Ga}_{1-x}\mathrm{N}} - E_{g,\mathrm{GaN}}\right], & \text{others}, \end{cases} \tag{4}$$

$$V(z,p)=\begin{cases} Q_j\left[E_{g,\mathrm{Al}_x\mathrm{Ga}_{1-x}\mathrm{N}}-E_{g,\mathrm{GaN}}\right], & \dfrac{L_w}{2}<|z|<\dfrac{L_b}{2},\\ 0, & |z|\le\dfrac{L_w}{2},\\ \infty, & |z|>\dfrac{L_b}{2}. \end{cases} \tag{5}$$

The wave function of an electron in the wurtzite GaN/$\mathrm{Al}_x\mathrm{Ga}_{1-x}\mathrm{N}$ QR can be written as [24]

$$\psi(\rho,\varphi,z)=f(\rho)\,h(z)\,e^{im\varphi},\quad m=0,\pm1,\pm2,\ldots$$

$$f(\rho)=\begin{cases} \dfrac{N_0J_0(\beta R_1)+Y_0(\beta R_1)}{I_0(\alpha R_1)}I_0(\alpha\rho), & \rho<R_1,\\ N_0J_0(\beta\rho)+Y_0(\beta\rho), & R_1\le\rho\le R_2,\\ \dfrac{N_0J_0(\beta R_1)+Y_0(\beta R_1)}{K_0(\alpha R_1)}K_0(\alpha\rho), & \rho>R_2, \end{cases} \tag{6}$$

where the constants (N_0, α, and β) are determined by the continuity of the derivative of the radial wave function at the QR boundary and m is the electron z-component angular momentum quantum number. The radial wave function $f(\rho)$ of the electron can be obtained using the Bessel function Y_m, J_m and the modified Bessel function I_m, K_m. The wave function $h(z)$ can be expressed by means of the Airy functions Ai and Bi

$$h(z)=\begin{cases} C_1\mathrm{Ai}(\varepsilon_1)+D_1\mathrm{Bi}(\varepsilon_1) & z<-\dfrac{L_w}{2}-L_b\\ C_2\mathrm{Ai}(\varepsilon_2)+D_2\mathrm{Bi}(\varepsilon_2) & -\dfrac{L_w}{2}-L_b<z<-\dfrac{L_w}{2}\\ C_3\mathrm{Ai}(\varepsilon_3)+D_3\mathrm{Bi}(\varepsilon_3) & |z|\le\dfrac{L_w}{2}\\ C_4\mathrm{Ai}(\varepsilon_4)+D_4\mathrm{Bi}(\varepsilon_4) & \dfrac{L_w}{2}<z<\dfrac{L_w}{2}+L_b\\ C_5\mathrm{Ai}(\varepsilon_5)+D_5\mathrm{Bi}(\varepsilon_5) & z>\dfrac{L_w}{2}+L_b, \end{cases} \tag{7}$$

where $\varepsilon_j=((2m_j^*/\hbar^2)eF)^{1/3}(z-E_z-V(z,p)/eF)$. The coefficients C_j and D_j ($j=1,2,3,4,$ and 5) can also be determined by the transfer matrix methods [20].

In order to calculate the donor binding energy, the trial wave function can be chosen as [6]

$$\phi(\rho,\varphi,z)=N\psi(\rho,\varphi,z)\,e^{-\alpha(\rho-\rho_0)^2-\beta(z-z_0)^2}, \tag{8}$$

where N is the normalization constant. With the adiabatic approximation, the donor binding energy of a hydrogenic impunity E_b is defined as the difference between the ground-state energy of the system without impurity and the ground-state energy of the system with impurity [26]; that is,

$$E_b=E_{0\rho}+E_{0z}-\min_{\alpha,\beta}\frac{\langle\psi\mid H\mid\psi\rangle}{\langle\psi\mid\psi\rangle}. \tag{9}$$

2.2. Pressure and Strain Dependence of Physical Parameters. In this model, we take the strains induced by the biaxial lattice mismatch into account. The components of biaxial stress tensors of GaN and AlGaN materials are given under the hydrostatic pressure P [33]

$$\begin{aligned} \varepsilon_{xx,\mathrm{GaN}}&=\varepsilon_{yy,\mathrm{GaN}}=\frac{a_{\mathrm{eq}}(p)-a_{\mathrm{GaN}}(P)}{a_{\mathrm{GaN}}(P)},\\ \varepsilon_{xx,\mathrm{AlGaN}}&=\varepsilon_{yy,\mathrm{AlGaN}}=\frac{a_{\mathrm{eq}}(p)-a_{\mathrm{AlGaN}}(P)}{a_{\mathrm{AlGaN}}(P)}, \end{aligned} \tag{10}$$

where the equilibrium lattice constant a_{eq} for the strained layer under the hydrostatic pressure P depends on the lattice constants of the component materials, and it is weighted by their relative thicknesses

$$a_{\mathrm{eq}}(p)=\frac{a_{\mathrm{GaN}}L_w+a_{\mathrm{GaAlN}}L_b}{L_w+L_b}. \tag{11}$$

The lattice constant a_ν of the material GaN(AlN) dependence of hydrostatic pressure [34] satisfies

$$a_\nu(P)=a_{0,\nu}\left(1-\frac{p}{3B_{0,\nu}}\right),\quad \nu=\mathrm{GaN},\mathrm{AlN}, \tag{12}$$

where the actual lattice constant a_{AlGaN} of the $\mathrm{Al}_x\mathrm{Ga}_{1-x}\mathrm{N}$ material can be obtained by the linear interpolation method from the corresponding values of GaN and AlN. The strain induced by the biaxial lattice mismatch along the z-direction in the heterostructure is [35]

$$\begin{aligned} \varepsilon_{zz,\mathrm{GaN}}&=R^H_{\mathrm{GaN}}\varepsilon_{xx,\mathrm{GaN}},\\ \varepsilon_{zz,\mathrm{AlGaN}}&=R^H_{\mathrm{AlGaN}}\varepsilon_{xx,\mathrm{AlGaN}}. \end{aligned} \tag{13}$$

The coefficient R^H_ν of the GaN (AlN) material is given by [35]

$$R^H_\nu=\frac{C_{11,\nu}(P)+C_{12,\nu}(P)-2C_{13,\nu}(P)}{C_{33,\nu}(P)-C_{13,\nu}(P)},\quad \nu=\mathrm{GaN},\mathrm{AlN}, \tag{14}$$

where $C_{\lambda\kappa,\nu}$ is the pressure-dependent elastic stiffness constant of material ν and is given by [36] $C_{\lambda\kappa,\nu}(P)=C_{\lambda\kappa,\nu}(0)+\sigma_{\lambda\kappa,\nu}P+\delta_{\lambda\kappa,\nu}P^2$. In addition, the coefficient R^H_{AlGaN} and the pressure-dependent elastic stiffness constant $C_{\lambda\kappa,\mathrm{AlGaN}}$ of the $\mathrm{Al}_x\mathrm{Ga}_{1-x}\mathrm{N}$ material can be obtained by the linear interpolation method from the corresponding values of GaN and AlN. The strain-dependent energy gaps of GaN and AlN are given by means of the following expression [37]:

$$\begin{aligned} E_{g,\mathrm{GaN}}=E_{g,\mathrm{GaN}}(p)&+2(a_{1,\mathrm{GaN}}+b_{1,\mathrm{GaN}})\varepsilon_{xx,\mathrm{GaN}}\\ &+(a_{2,\mathrm{GaN}}+b_{2,\mathrm{GaN}})\varepsilon_{zz,\mathrm{GaN}}, \end{aligned} \tag{15a}$$

$$E_{g,\mathrm{AlN}}=E_{g,\mathrm{AlN}}(p)+2a_{1,\mathrm{AlN}}\varepsilon_{xx,\mathrm{AlN}}+a_{2,\mathrm{AlN}}\varepsilon_{zz,\mathrm{AlN}}, \tag{15b}$$

where $a_{1,\nu}$, $a_{2,\nu}$, $b_{1,\nu}$, and $b_{2,\nu}$ (ν = GaN and AlN) are the deformation potentials. The dependence of the energy gap

$E_{g,\nu}$ on hydrostatic pressure P is considered by the following equation [38]:

$$E_{g,\nu}(p) = E_{g,\nu}(0) + \chi_\nu p. \tag{16}$$

The energy gap of the $Al_xGa_{1-x}N$ alloy can be calculated from energy gaps of GaN and AlN with the simplified coherent potential approximation (SCPA) [39]:

$$E_{g,\mathrm{AlGaN}} = \frac{E_{g,\mathrm{GaN}}E_{g,\mathrm{AlN}}}{xE_{g,\mathrm{GaN}} + (1-x)E_{g,\mathrm{AlN}}}. \tag{17}$$

The biaxial strain and hydrostatic pressure dependence of the electron effective masses in the radial direction and the z-direction can be calculated by [40]

$$\frac{m_0}{m_\nu^{\perp,/\!/}(p)} = 1 + \frac{C_{j,\nu}}{E_{g,\nu}(p)}, \tag{18}$$

where $C_{j,\nu}$ is a fixed value for a given material ν and can be derived from the values of $m_\nu^{\perp,/\!/}(0)$ and $E_{g,\nu}(0)$. The electron effective mass of the $Al_xGa_{1-x}N$ material can be obtained by the linear interpolation method from the corresponding values of GaN and AlN. In (5), considering the biaxial and uniaxial strain and hydrostatic pressure effects, the dielectric constants and the phonon eigenfrequencies will be changed. The static dielectric constant ε_ξ in material ν can be derived from the generalized Lyddane-Sachs-Teller relation [35]

$$\varepsilon_\xi^\nu(p) = \varepsilon_{\infty,\xi}^\nu(p)\left(\frac{\omega_{\mathrm{LO},\xi}^\nu(P)}{\omega_{\mathrm{TO},\xi}^\nu(P)}\right)^2, \tag{19}$$

where the LO- and TO-phonon frequencies influenced by biaxial strain and hydrostatic pressure can be written as [35]

$$\omega_{j,\xi}^\nu = \omega_{j,\xi}^\nu(p) + 2K_{j,\xi,xx}^\nu\varepsilon_{xx,\nu}(p) + K_{j,\xi,zz}^\nu\varepsilon_{zz,\nu}(p). \tag{20}$$

Furthermore, the hydrostatic pressure dependence of ω_j can be determined by the given mode-Grüneisen parameters [41]

$$\gamma_{j,\xi}^\nu = B_{0,\nu}\frac{1}{\omega_{j,\xi}^\nu(0)}\left(\frac{\partial\omega_{j,\xi}^\nu(p)}{\partial p}\right), \tag{21}$$

where the subscript j represents LO- or TO-phonon, ξ ($\xi = \perp$ or z) denotes x–y plane or z-direction, $\omega_{j,\xi}^\nu(0)$ is the zone-center phonon frequency of material ν, $\gamma_{j,\xi}^\nu$ is Grüneisen parameter of phonon mode given in [35], B_0 is bulk modulus, and $K_{j,\xi,xx}^\nu$ and $K_{j,\xi,zz}^\nu$ are the strain coefficients of zone-center phonon modes.

Following [14], considering the influence of hydrostatic pressure, the high frequency dielectric constants in (19) can be written as

$$\frac{\partial\varepsilon_{\infty,\xi}^\nu(p)}{\partial p} = -\frac{5\left(\varepsilon_{\infty,\xi}^\nu - 1\right)}{3B_{0,\nu}}\left(0.9 - f_{\mathrm{ion}}^\nu\right), \tag{22}$$

where f_{ion}^ν (ν = GaN and AlN) is the Phillips iconicity parameter of material ν and $B_{0,\nu}$ is the static bulk modulus under hydrostatic pressure and is given by [41]

$$B_{0,\nu} = \frac{\left(C_{11,\nu}(P) + C_{12,\nu}(P)\right)C_{33,\nu}(P) - 2C_{13,\nu}^2(P)}{C_{11,\nu}(P) + C_{12,\nu}(P) + 2C_{33,\nu}(P) - 4C_{13,\nu}(P)}, \tag{23}$$

where $C_{11,\nu}$, $C_{12,\nu}$, $C_{13,\nu}$, and $C_{33,\nu}$ are the elastic constants of material ν.

The effective mean relative dielectric constant in (1) is defined as [39]

$$\overline{\varepsilon_\nu}(p) = \frac{2}{3}\varepsilon_\xi^\nu(p) + \frac{1}{3}\varepsilon_\xi^\nu(p), \quad (\xi = \perp \text{ or } z). \tag{24}$$

The piezoelectric polarization along the [0001]-oriented wurtzite $GaN/Al_xGa_{1-x}N$ QR can be calculated as [14]

$$P_{pe}^\nu = e_{33}^\nu(p)\varepsilon_{zz}^\nu + 2e_{31}^\nu(p)\varepsilon_{xx}^\nu, \tag{25}$$

where e_{31}^ν and e_{33}^ν are the pressure-dependent piezoelectric constants of material ν and are given by [14]

$$e_{31}^\nu(p) = e_{31}^\nu(0) + \frac{4eZ_\nu^*}{\sqrt{3}a_\nu^2(p)}\frac{du}{d\varepsilon_{xx,\nu}}, \tag{26a}$$

$$e_{33}^\nu(p) = e_{33}^\nu(0) + \frac{4eZ_\nu^*}{\sqrt{3}a_\nu^2(p)}\frac{du}{d\varepsilon_{zz,\nu}}. \tag{26b}$$

Here, Z_ν^* is the Born effective charge, $a_{0,\nu}$ is the pressure-dependent equilibrium lattice constant, and u is the anion-cation bond length along the [0001]-direction in units of c. Based on the definition of the strain tensor and the bulk modulus, we can derive the following formula for the pressure dependence of the QR inner (outer) radius $R_i(P)$, the height $L_w(P)$ of the QR, and the thickness of barrier $L_b(P)$ along the QR growth direction:

$$R_i(P) = R_i\left(1 - 2(S_{11,i} + 2S_{12,i})P\right)^{1/2}, \quad i = 1, 2 \tag{27a}$$

$$L_w(P) = L_w\left(1 - 2\left(S_{11,w} + 2S_{12,w}\right)P\right), \tag{27b}$$

$$L_b(P) = L_b\left(1 - 2\left(S_{11,b} + 2S_{12,b}\right)P\right), \tag{27c}$$

where R_i, L_w, and L_b are the QR inner (outer) radius, the QR height, and the thickness of the barrier layer along the QR growth direction at zero pressure, respectively. $S_{11,i}$ and $S_{12,i}$ are the compliance constants of GaN and $Al_xGa_{1-x}N$ materials, respectively [42].

3. Results and Discussions

Considering the effects of the hydrostatic pressure and strong built-in electric field due to the spontaneous and piezoelectric polarizations, we calculated the donor binding energy of a hydrogenic impurity E_b as a function of structural parameters, such as inner radius R_1, outer radius R_2, height L_w, and impurity position z_0 along the growth direction z-axis in cylindrical wurtzite $GaN/Al_xGa_{1-x}N$ QR. All material parameters used in our calculations are listed in Tables 1–4. The $Al_xGa_{1-x}N$ material parameters can be calculated from the corresponding parameters of GaN and AlN by using a linear interpolation (Vegard' slaw). In this paper, the Al concentration x is 0.15.

Figure 2 displays the built-in electric field (BEF) F_{GaN} (F_{AlGaN}) as a function of the hydrostatic pressure P for different QR heights L_w with barrier thickness (L_b = 30 nm)

Table 1: Lattice constant a (in units of nm), effective mass m_e (in units of a free-electron mass m_0), piezoelectric constants e_{31} and e_{33} (in units of C/m^2), and deformation potentials a_1, a_2, b_1, and b_2 (in units of eV).

	a	$m_\perp$	$m_{//}$	e_{31}	e_{33}	a_1	b_1	a_2	b_2
GaN	0.3189[a]	0.18[a]	0.2[a]	−0.34[b]	0.67[b]	−4.09[c]	−8.87[c]	−7.02[c]	3.65[c]
AlN	0.3112[a]	0.25[a]	0.33[a]	−0.53[b]	1.50[b]	−3.39[c]	−11.81[c]	−9.42[c]	4.02[c]

[a]Reference [14], [b]reference [36], [c]reference [35].

Table 2: Band gaps E_g (in units of eV), spontaneous polarization (in units of C/m^2), elastic constants C_{11}, C_{12}, C_{13}, and C_{33} (in units of GPa), Phillips iconicity parameter f_{ion}, and the high frequency dielectric constant ε_∞.

	E_g	p^{sp}	C_{11}	C_{12}	C_{13}	C_{33}	f_{ion}	$\varepsilon_{\infty,\perp}$	$\varepsilon_{\infty,z}$
GaN	3.507[a]	−0.034[a]	390[b]	145[b]	106[b]	398[b]	0.5[a]	5.20[a]	5.39[a]
AlN	6.230[a]	−0.090[a]	398[b]	140[b]	127[b]	382[b]	0.499[a]	4.30[a]	4.52[a]

[a]Reference [7], [b]reference [36].

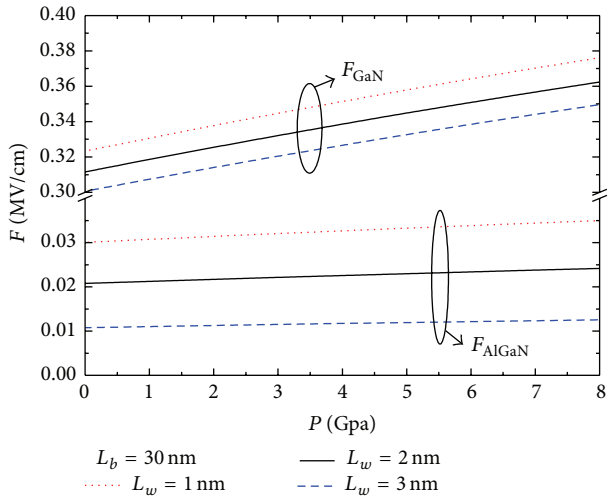

Figure 2: The built-in electric field F_{GaN} (F_{AlGaN}) in the ring (barrier) layer along the QR growth direction as a function of the hydrostatic pressure P in cylindrical wurtzite GaN/Al$_x$Ga$_{1-x}$N strained QR with different QR heights.

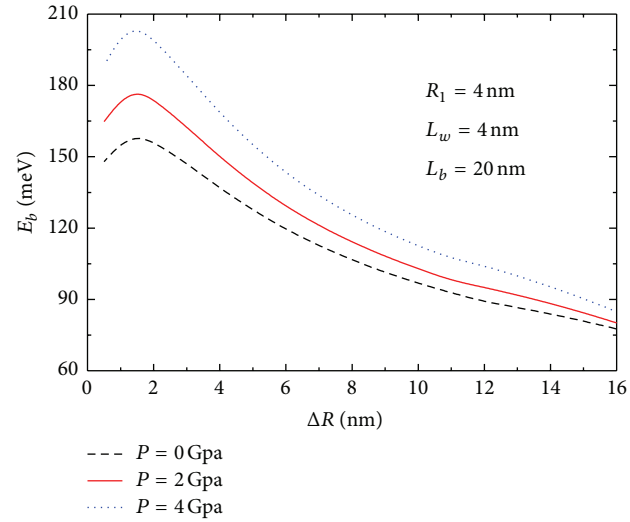

Figure 3: The ground-state donor binding energy in cylindrical wurtzite GaN/Al$_x$Ga$_{1-x}$N strained QR as a function of the radial thickness (ΔR) for $R_1 = 4$ nm, $L_w = 4$ nm, $L_b = 20$ nm, and several values of the hydrostatic pressure.

in wurtzite GaN/Al$_x$Ga$_{1-x}$N strained QR. Numerical results show that the BEF F_{GaN} (F_{AlGaN}) increases linearly with increasing the hydrostatic pressure P. For example, when the hydrostatic pressure P increases from 0 to 8 GPa, the BEF F_{GaN} (F_{AlGaN}) increases to 0.23 (0.024) MV/cm. For a given pressure and barrier thickness, Figure 2 also shows that the BEF F_{GaN} (F_{AlGaN}) increases as the height L_w decreases and the BEF F_{AlGaN} remains insensitive to the variation of the hydrostatic pressure. This is caused by the change of the pressure-dependent piezoelectric constants, the biaxial strains, the dielectric constants, and the structural parameters of wurtzite GaN/Al$_x$Ga$_{1-x}$N strained QR. According to (11), the equilibrium lattice constant a_{eq} of the strained layer increases with decreasing the QR height L_w. Thus, the absolute value of the strain tensor $\varepsilon_{xx,\text{GaN}}$ of the ring layer along the QR growth direction increases, which induces the fact that the strength of the built-in electric field F_w increases with the decrement of the height L_w; this can be understood based on (3).

In Figure 3, the ground-state donor binding energy in cylindrical wurtzite GaN/Al$_x$Ga$_{1-x}$N QR is shown as a function of the radial thickness ΔR with the parameters $R_1 = 4$ nm, $L_w = 4$ nm, and $L_b = 20$ nm for different hydrostatic pressures ($p = 0$ Gpa, 2 Gpa, 4 Gpa). The impurity is placed at the center of the QR. Set $\rho_0 = (R_1 + R_2)/2$ and $z_0 = 0$. As shown in Figure 3, the donor binding energy increases with decreasing the radial thickness (ΔR) in all cases, reaches a maximum value, and then decreases sharply. The behavior is related to the variation of the electron confinement in QR; the electron wave function is more firmly localized inside the QR with the decrease of the QR radial thickness. Thus, the Coulomb interaction between the electron and the impurity ion is enhanced and the donor binding energy increases correspondingly. However, when the radial thickness decreases continuously to a certain value, the kinetic energy of the confined electron raises greatly, which increases greatly the probability of the electron penetrating into the

Table 3: Strain coefficients of the zone-center phonon modes $K^{\nu}_{j,\xi,xx}$ and $K^{\nu}_{j,\xi,zz}$ (in units of cm^{-1}).

	$K_{\mathrm{To},\perp,xx}$	$K_{\mathrm{To},z,xx}$	$K_{\mathrm{To},\perp,zz}$	$K_{\mathrm{To},\perp,zz}$	$K_{\mathrm{Lo},\perp,xx}$	$K_{\mathrm{Lo},z,xx}$	$K_{\mathrm{Lo},\perp,zz}$	$K_{\mathrm{Lo},\perp,zz}$
GaN	−1139[a]	−931[a]	−300[a]	−443[a]	−1198[a]	−885[a]	−389[a]	−618[a]
AlN	−1208[a]	−1330[a]	−391[a]	−70[a]	−1233[a]	−1038[a]	−442[a]	−434[a]

[a]Reference [14].

Table 4: Band gap pressure coefficients χ (meV/GPa), Born effective charges Z^*, and phonon frequencies ω_{Lo} and ω_{To} (cm^{-1}).

	χ	Z^*	$\mathrm{du}/\mathrm{d}\varepsilon_{xx}$	$\mathrm{du}/\mathrm{d}\varepsilon_{zz}$	$\omega_{\mathrm{Lo},\perp}$	$\omega_{\mathrm{Lo},z}$	$\omega_{\mathrm{To},\perp}$	$\omega_{\mathrm{To},z}$
GaN	39[a]	1.18[b]	0.262[b]	−0.208[b]	757[b]	748[b]	568[b]	540[b]
AlN	40[a]	1.27[b]	0.308[b]	−0.242[b]	924[b]	898[b]	677[b]	318[b]

[a]Reference [43], [b]reference [39].

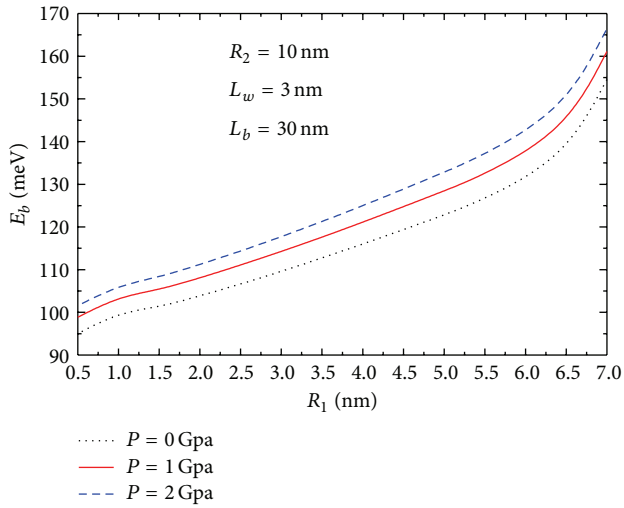

Figure 4: The ground-state donor binding energy in cylindrical wurtzite $GaN/Al_xGa_{1-x}N$ strained QR as a function of the QR inner radius (R_1) for $R_2 = 10$ nm, $L_w = 3$ nm, $L_b = 30$ nm, and several values of the hydrostatic pressure.

potential barrier by the uncertainty principle. Therefore, the donor binding energy starts decreasing quickly due to the weakness of the geometrical confinement in the radial direction. Moreover, Figure 3 also displays that the stronger the applied hydrostatic pressures is, the bigger the donor binding energy is. It can be explained that the QR sizes become small gradually with the larger hydrostatic pressure, and much stronger quantum confinement effect results in an increase of the donor binding energy.

In Figure 4, we present the ground-state donor binding energy in cylindrical wurtzite $GaN/Al_xGa_{1-x}N$ strained QR as a function of the inner radius with the parameters (R_2 = 10 nm, $L_w = 3$ nm, and $L_b = 30$ nm) for different hydrostatic pressures ($p = 0$ Gpa, 1 Gpa, 2 Gpa). The impurity is placed at the center of the QR. Set $\rho_0 = (R_1 + R_2)/2$ and $z_0 = 0$. For a fixed value of the outer radius, the QR radial thickness ($R_2 - R_1$) decreases as the inner radius augments; hence, the size quantization becomes stronger which leads to an increase in the donor binding energy. It can be understood that the expectation value of the electron-impurity distance along the radial direction decreases with the strengthening of the size quantization, and the probability of the electron localized near the impurity ion increases greatly; therefore, the donor binding energy becomes larger. The curves in Figure 6 also show that the donor binding energy increases quickly with the inner radius $R_1 \geq 6$ nm. It is because the localization effect of the electron around the impurity ion is caused mainly by the radial confining potential and the influences of the hydrostatic pressure on the Coulomb interaction between the electron and the impurity ion are weaker; therefore, the donor binding energy increases gradually as the radial thickness ΔR becomes narrow. In addition, for a given structure parameters of the QR the stronger the applied hydrostatic pressure is, the bigger the donor binding energy is. This can be explained by the fact that a growth in the hydrostatic pressure leads to the increase in the quantum localization effect of the electron wave function.

To clarify the effect of the applied hydrostatic pressure on the ground-state donor binding energy, we investigated the ground-state donor binding energy in cylindrical wurtzite $GaN/Al_xGa_{1-x}N$ strained QR with the parameters (R_1 = 5 nm, R_2 = 15 nm, L_b = 20 nm, and $\rho_0 = (R_1 + R_2)/2$, $z_0 = 0.0a^*$) and several values of the QR height L_w. From Figure 5, one can observe that the donor binding energy increases almost linearly as the hydrostatic pressure P increases. The behavior can be explained as follows. Firstly, the changes of the pressure-dependent piezoelectric constants, biaxial strains, and dielectric constants can cause the modification of the polarization in the ring layer, which leads to a significant increase of the BEF F_{GaN}. Secondly, the bigger hydrostatic pressure leads to an increase in the electron effective masses, which can cause the increment of the electron confinement potential in z-direction. At last, the bigger hydrostatic pressure can also lead to the decrement of the expected value of the distance between the electron and the impurity ion. Therefore, the larger the applied hydrostatic pressure is, the stronger the Coulomb interaction between the electron and the impurity is, and the donor binding energy increases correspondingly. Taking the solid curve for example, for the QR height $L_w = 3$ nm, the donor binding energy increases 24 meV approximately if the hydrostatic pressure P increases from 0 to 8 GPa. Thus, the applied hydrostatic

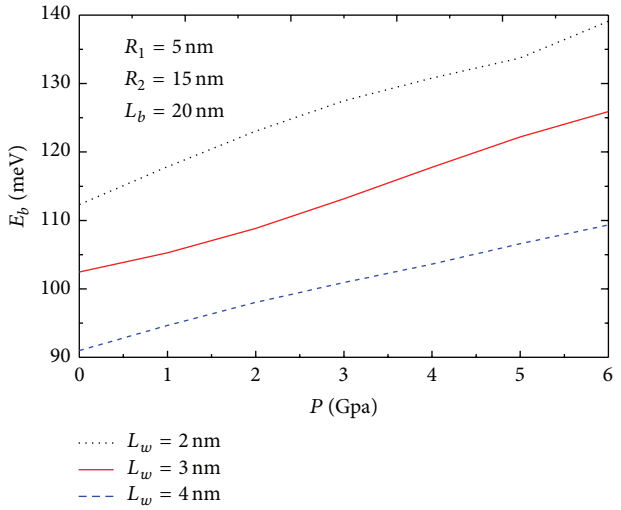

Figure 5: The ground-state donor binding energy in cylindrical wurtzite GaN/$Al_xGa_{1-x}N$ strained QR as a function of the hydrostatic pressure (P) for R_1 = 5 nm, R_2 = 15 nm, L_b = 20 nm, and several values of the QR height L_w.

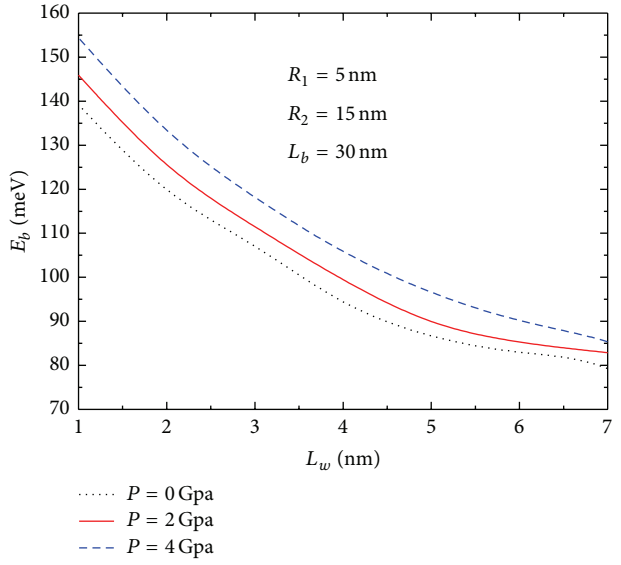

Figure 6: The ground-state donor binding energy in cylindrical wurtzite GaN/$Al_xGa_{1-x}N$ strained QR as a function of the QR height L_w for R_1 = 5 nm, R_2 = 15 nm, L_b = 20 nm, and several values of the hydrostatic pressure (P).

pressure has an important influence on the donor binding energy. Figure 6 displays the ground-state donor binding energy as a function of cylindrical wurtzite GaN/$Al_xGa_{1-x}N$ strained QR height L_w with the parameters (R_1 = 5 nm, R_2 = 15 nm, L_b = 30 nm, and $\rho_0 = (R_1 + R_2)/2$, $z_0 = 0.0a^*$) and several values of the applied hydrostatic pressure. We can see from Figure 6 that the donor binding energy increases monotonically as the height L_w decreases from 7 nm to 1 nm in all case. As expected, the electron wave function is much strongly compressed in the QR for the less height of the QR, and the electron-impurity interaction becomes stronger,

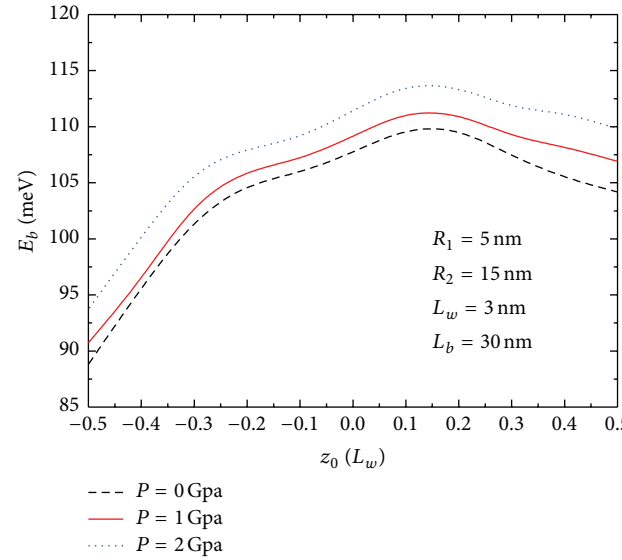

Figure 7: The ground-state donor binding energy in cylindrical wurtzite GaN/$Al_xGa_{1-x}N$ strained QR as a function of the axial impurity position z_0 for R_1 = 5 nm, R_2 = 15 nm, L_w = 3 nm, L_b = 30 nm, and several values of the hydrostatic pressure (P).

which leads to the enhancement of the binding energy correspondingly. Figure 6 also shows that the donor binding energy increases with the increment of the hydrostatic pressure P. This is because the quantum localization effect of the electron wave function in wurtzite GaN/$Al_xGa_{1-x}N$ strained QR is strengthened with the increase of the applied hydrostatic pressure. Therefore, the decrement of the mean relative electron-impurity distance leads to the increase in the donor binding energy with the same spatial confinement.

In Figure 7, the ground-state donor binding energy is investigated as a function of the impurity position z_0 along the QR growth direction with the parameters (R_1 = 5 nm, R_2 = 15 nm, d = 3 nm, and $\rho_0 = (R_1 + R_2)/2$) and several values of the applied hydrostatic pressure (P = 0, 1, 2 Gpa). It is seen that the curves in Figure 7 are absolutely asymmetric, and the donor binding energy firstly increases, reaches a maximum value, and then decreases gradually when the impurity is moved from the plane $z = -L_w/2$ to the plane $L_w/2$ along the QR growth direction. The maximum value of the donor binding energy is not located at the point $[(R_1 + R_2)/2, 0]$ and shifted towards positive z-direction. It is because the topology structure of the QR and the strong BEF modify the spread of the electron wave function in the QR. The direction of the built-in electric field F_w in the ring layer is opposite to the QR growth direction. Thus, the built-in electric field F_w pushes the electron towards positive z-direction. This behavior is in agreement with the result of [19]. In addition, the larger the applied hydrostatic pressure is, the stronger the localization effect of the electron wave function is with the same parameters (L_w, ΔR, and ρ_0), so that the peak value of the donor binding energy increases accordingly. Therefore, the distribution of the electron wave function is not central symmetrical about the QR in presence of the strong BEF.

4. Conclusions

With the framework of the effective mass approximation, the ground-state donor binding energies in cylindrical wurtzite $GaN/Al_xGa_{1-x}N$ strained QR are investigated theoretically in the presence of built-in electric field and hydrostatic pressure by means of a variational approach. The ground-state donor binding energy depends strongly on ring geometry, applied hydrostatic pressure, and impurity position in the finite confinement potential. Numerical results show that the donor binding energy increases firstly, reaches a maximum value, and then drops quickly as the radial thickness of the QR decreases. The donor binding energy is an increasing (a decreasing) function of inner radius (height). In addition, the donor binding energy has a maximum when the impurity ion is moved along the z-axis of the QR from the bottom of the QR to the top. Moreover, the stronger the applied hydrostatic pressure is, the bigger the peak value of the impurity binding energy is, with the same spatial confinement. And the position of the peak value of the binding energy is also shifted towards positive z-direction. The electronic wave function distribution in the QR is also obviously modified by the applied hydrostatic pressure. These theoretical results obtained in this paper are useful for design of some photoelectric devices constructed based on $GaN/Al_xGa_{1-x}N$ QR structures.

Conflict of Interests

The authors declare that there is no conflict of interests regarding the publication of this paper.

Acknowledgments

This work was supported by the Scientific and Technological Department Foundation of Hebei Province (no. 12210617) and the Natural Science Foundation of Hebei Province (no. A201420308).

References

[1] S. Nakamura, M. Senoh, S. Nagahama et al., "Violet InGaN/GaN/AlGaN-based laser diodes operable at 50°C with a fundamental transverse mode," *Japanese Journal of Applied Physics*, vol. 38, part 2, pp. L226–L229, 1999.

[2] S. Nakamura and S. F. Chichibu, *Introduction to Nitride Semiconductor Blue Lasers and Light Emitting Diodes*, Taylor & Francis, London, UK, 2000.

[3] S.-H. Han, D.-Y. Lee, S.-J. Lee et al., "Effect of electron blocking layer on efficiency droop in InGaN/GaN multiple quantum well light-emitting diodes," *Applied Physics Letters*, vol. 94, no. 23, Article ID 231123, 3 pages, 2009.

[4] M. Zhang and S.-L. Ban, "Pressure influence on the Stark effect of impurity states in a strained wurtzite $GaN/Al_xGa_{1-x}N$ heterojunction," *Chinese Physics B*, vol. 18, no. 10, pp. 4449–4455, 2009.

[5] M. Pattammal and A. J. Peter, "Electronic states of a hydrogenic impurity in a zinc-blende GaN/AlGaN quantum well," *Applied Surface Science*, vol. 256, no. 22, pp. 6748–6752, 2010.

[6] C. X. Xia, Z. P. Zeng, S. Y. Wei, and J. B. Wei, "Shallow-donor impurity in vertical-stacked InGaN/GaN multiple-quantum wells: electric field effect," *Physica E*, vol. 43, no. 1, pp. 458–461, 2010.

[7] M. Zhang and S.-L. Ban, "Screening influence on the Stark effect of impurity states in strained wurtzite $GaN/AI_xGa_{1-x}N$ heterojunctions under pressure," *Chinese Physics B*, vol. 18, no. 12, pp. 5437–5442, 2009.

[8] Y. N. Wei, Y. Ji, Q. Sun, C. X. Xia, and Y. Jia, "Barrier width and built-in electric field effects on hydrogenic impurity in wurtzite GaN/AlGaN quantum well," *Physica E*, vol. 44, no. 2, pp. 511–514, 2011.

[9] H. E. Ghazi, A. Jorio, and I. Zorkani, "Pressure-dependent shallow donor binding energy in InGaN/GaN square QWWs," *Physica B*, vol. 410, no. 1, pp. 49–52, 2013.

[10] P. Baser, S. Elagoz, and N. Baraz, "Hydrogenic impurity states in zinc-blende $In_xGa_{1-x}N/GaN$ in cylindrical quantum well wires under hydrostatic pressure," *Physica E*, vol. 44, no. 2, pp. 356–360, 2011.

[11] C. X. Xia, Z. P. Zeng, and S. Y. Wei, "Effects of applied electric field and hydrostatic pressure on donor impurity states in cylindrical GaN/AlN quantum dot," *Journal of Applied Physics*, vol. 107, no. 1, Article ID 014305, 2010.

[12] M. Kırak, S. Yılmaz, M. Şahin, and M. Gençaslan, "The electric field effects on the binding energies and the nonlinear optical properties of a donor impurity in a spherical quantum dot," *Journal of Applied Physics*, vol. 109, no. 9, Article ID 094309, 8 pages, 2011.

[13] M. Zhang and J.-J. Shi, "Influence of pressure on exciton states and interband optical transitions in wurtzite InGaN/GaN coupled quantum dot nanowire heterostructures with polarization and dielectric mismatch," *Journal of Applied Physics*, vol. 111, Article ID 113516, 11 pages, 2012.

[14] D. M. Zheng, Z. C. Wang, and B. Q. Xiao, "Effects of hydrostatic pressure on ionized donor bound exciton states in strained wurtzite $GaN/Al_xGa_{1-x}N$ cylindrical quantum dots," *Physica B*, vol. 407, no. 21, pp. 4160–4167, 2012.

[15] M. G. Barseghyan, A. A. Kirakosyan, and C. A. Duque, "Hydrostatic pressure,electric and magnetic field effects on shallow donor impurity states and photoionization cross section in cylindrical GaAs-$Ga_{1-x}Al_xAs$ quantum dots," *Physica Status Solidi (B) Basic Research*, vol. 246, no. 3, pp. 626–629, 2009.

[16] J. M. Ferreyra and C. R. Proetto, "Strong-confinement approach for impurities in quantum dots," *Physical Review B*, vol. 52, no. 4, Article ID R2309, pp. 1–7, 1995.

[17] J. M. Ferreyra, P. Bosshard, and C. R. Proetto, "Strong-confinement approach for impurities in parabolic quantum dots," *Physical Review B*, vol. 55, no. 20, pp. 13682–13688, 1997.

[18] C. Bose and C. K. Sarkar, "Perturbation calculation of donor states in a spherical quantum dot," *Solid-State Electronics*, vol. 42, no. 9, pp. 1661–1663, 1998.

[19] C. X. Xia, S. Y. Wei, and X. Zhao, "Built-in electric field effect on hydrogenic impurity in wurtzite GaN/AlGaN quantum dot," *Applied Surface Science*, vol. 253, no. 12, pp. 5345–5348, 2007.

[20] H. Wu, H. Wang, L. Jiang, Q. Gong, and S. Feng, "The electric field effect on binding energy of hydrogenic impurity in zinc-blende $GaN/Al_xGa_{1-x}N$ spherical quantum dot," *Physica B*, vol. 404, no. 1, pp. 122–126, 2009.

[21] C. X. Xia, T. X. Wang, and S. Y. Wei, "Pressure effects on the donor binding energy in zinc-blende InGaN/GaN quantum dot," *Superlattices and Microstructures*, vol. 46, no. 6, pp. 840–845, 2009.

[22] Z. Gong, Z. C. Niu, S. S. Huang, Z. D. Fang, B. Q. Sun, and J. B. Xia, "Formation of GaAs/AlGaAs and InGaAs/GaAs nanorings by droplet molecular-beam epitaxy," *Applied Physics Letters*, vol. 87, no. 9, Article ID 093116, 2005.

[23] M. Dejarld, K. Reyes, P. Smereka, and J. M. Millunchick, "Mechanisms of ring and island formation in lattice mismatched droplet epitaxy," *Applied Physics Letters*, vol. 102, no. 13, Article ID 133107, 2013.

[24] S.-S. Li and J.-B. Xia, "Electronic states of InAs/GaAs quantum ring," *Journal of Applied Physics*, vol. 89, no. 6, pp. 3434–3437, 2001.

[25] S. S. Li and J. B. Xia, "Electronic structures of GaAs/$Al_xGa_{1-x}As$ quantum double rings," *Nanoscale Research Letters*, vol. 1, no. 1, pp. 167–171, 2006.

[26] Z. Barticevic, M. Pacheco, and A. Latgé, "Quantum rings under magnetic fields: electronic and optical properties," *Physical Review B*, vol. 62, no. 11, pp. 6963–6966, 2000.

[27] A. Bruno-Alfonso and A. Latgé, "Semiconductor quantum rings: shallow-donor levels," *Physical Review B*, vol. 61, no. 23, pp. 15887–15894, 2000.

[28] H. M. Baghramyan, M. G. Barseghyan, C. A. Duque, and A. A. Kirakosyan, "Binding energy of hydrogenic donor impurity in GaAs/$Ga_{1-x}Al_xAs$ concentric double quantum rings: effects of geometry, hydrostatic pressure, temperature, and aluminum concentration," *Physica E*, vol. 48, no. 1, pp. 164–170, 2013.

[29] B. S. Monozon and P. Schmelcher, "Impurity center in a semiconductor quantum ring in the presence of crossed magnetic and electric fields," *Physical Review B: Condensed Matter and Materials Physics*, vol. 67, no. 4, Article ID 045203, 14 pages, 2003.

[30] M. G. Barseghyan, M. E. Mora-Ramos, and C. A. Duque, "Hydrostatic pressure, impurity position and electric and magnetic field effects on the binding energy and photo-ionization cross section of a hydrogenic donor impurity in an InAs Pöschl-Teller quantum ring," *The European Physical Journal B*, vol. 84, no. 2, pp. 265–271, 2011.

[31] M. G. Barseghyan, A. Hakimyfard, A. A. Kirakosyan, M. E. Mora-Ramos, and C. A. Duque, "Hydrostatic pressure and electric and magnetic field effects on the binding energy of a hydrogenic donor impurity in InAs Pöschl-Teller quantum ring," *Superlattices and Microstructures*, vol. 51, no. 1, pp. 119–127, 2012.

[32] G. X. Wang, X. Z. Duan, and W. Chen, "Hydrogenic-donor impurity binding energy dependence of the electric field in GaAs/$Al_xGa_{1-x}As$ quantum rings," *Journal of Nanomaterials*, vol. 2013, Article ID 240563, 7 pages, 2013.

[33] F. J. Culchac, N. Porras-Montenegro, and A. Latǵ, "Hydrostatic pressure effects on electron states in GaAs-(Ga,Al)As double quantum rings," *Journal of Applied Physics*, vol. 105, no. 9, Article ID 094324, 2009.

[34] S. Kalliakos, P. Lefebvre, and T. Taliercio, "Nonlinear behavior of photoabsorption in hexagonal nitride quantum wells due to free carrier screening of the internal fields," *Physical Review B—Condensed Matter and Materials Physics*, vol. 67, Article ID 205307, pp. 1–6, 2003.

[35] J.-M. Wagner and F. Bechstedt, "Pressure dependence of the dielectric and lattice-dynamical properties of GaN and AlN," *Physical Review B*, vol. 62, no. 7, pp. 4526–4534, 2000.

[36] S. P. Łepkowski, J. A. Majewski, and G. Jurczak, "Nonlinear elasticity in III-N compounds: *Ab initio* calculations," *Physical Review B*, vol. 72, Article ID 245201, 6 pages, 2005.

[37] S. R. Lee, A. F. Wright, M. H. Crawford, G. A. Petersen, J. Han, and R. M. Biefeld, "The band-gap bowing of $Al_xGa_{1-x}N$ alloys," *Applied Physics Letters*, vol. 74, no. 22, pp. 3344–3346, 1999.

[38] N. E. Christensen and I. Gorczyca, "Optical and structural properties of III-V nitrides under pressure," *Physical Review B*, vol. 50, no. 7, pp. 4397–4415, 1994.

[39] J.-M. Wagner and F. Bechstedt, "Properties of strained wurtzite GaN and AlN: Ab initio studies," *Physical Review B—Condensed Matter and Materials Physics*, vol. 66, no. 11, Article ID 115202, pp. 1–20, 2002.

[40] D. Z.-Y. Ting and Y.-C. Chang, "Γ-X mixing in GaAs/$Al_xGa_{1-x}As$ and $Al_xGa_{1-x}As$/AlAs superlattices," *Physical Review B*, vol. 36, no. 8, pp. 4359–4374, 1987.

[41] P. Perlin, L. Mattos, N. A. Shapiro et al., "Reduction of the energy gap pressure coefficient of GaN due to the constraining presence of the sapphire substrate," *Journal of Applied Physics*, vol. 85, no. 4, pp. 2385–2389, 1999.

[42] N. Raigoza, C. A. Duque, N. Porras-Montenegro, and L. E. Oliveira, "Correlated electron-hole transition energies in quantum-well wires: effects of hydrostatic pressure," *Physica B*, vol. 371, no. 1, pp. 153–157, 2006.

[43] N. E. Christensen and I. Gorczyca, "Optical and structural properties of III-V nitrides under pressure," *Physical Review B*, vol. 50, no. 7, pp. 4397–4415, 1994.